J. Phys.: Condens. Matter **9** (1997) 10829–10842. Printed in the UK PII: S0953-8984(97)87035-X

Determination of optical activity in monoclinic crystals of tartaric acid, $(2R, 3R)$-(+)-$C_4H_6O_6$, using the 'tilter' method

D Mucha†, K Stadnicka†, W Kaminsky‡ and A M Glazer‡

† Faculty of Chemistry, Jagiellonian University, ul. Ingardena 3, 30-060 Cracow, Poland
‡ Clarendon Laboratory, University of Oxford, Parks Road, Oxford OX1 3PU, UK

Received 19 August 1997

Abstract. The complete optical-gyration tensor for a monoclinic crystal of $(2R, 3R)$-(+)-$C_4H_6O_6$ has been determined by the tilter method at a wavelength of 680 nm. The tensor components in terms of rotatory power in relation to the principal axes of the indicatrix were found to be $\rho_{11}^{\circ} = 79(7)$, $\rho_{22}^{\circ} = 90(13)$, $\rho_{33}^{\circ} = -70(4)$, $\rho_{23}^{\circ} = -18(8)^{\circ}$ mm^{-1} with $\rho = -12.3(1.0)^{\circ}$ mm^{-1} in the optic-axis directions. The absolute optical chirality has also been established by combining the structural chirality determination (through the x-ray anomalous scattering) and the signs of the gyration tensor components measured for the same crystal.

1. Introduction

Although the first description of tartaric acid (TA) ((+)-$C_4H_6O_6$) crystals was given in 1841 by De la Provostaye and the link between crystal habit and optical rotation of its aqueous solution was established by Pasteur (1849), the absolute structure of TA crystals was determined no earlier than in 1972 by Hope and de la Camp (space group $P2_1$).

TA crystals were discovered to be strongly piezoelectric (Curie and Curie 1882) and optically active (Dufet 1907) with a moderate rotatory power of about $\pm 11.4^{\circ}$ mm^{-1} observed along the optic axis for 589 nm. Optical rotatory dispersion (ORD) was first established by Longchambon (1924), but a complete optical-gyration tensor has never been determined, as the low symmetry of this crystal makes this rather difficult. The symmetric axial tensor of monoclinic crystal class 2 consists of four independent components: $\rho_{11}, \rho_{22}, \rho_{33}, \rho_{13} = \rho_{31}$ and only one direction ρ_{22} is fixed by 2-fold symmetry. Moreover, along directions different from the optic axes, the optical rotation is dominated by high linear birefringence. Thus, to measure optical rotation in birefringent directions, a special technique should be used, for example the HAUP-system developed by Kobayashi and Uesu (1983). However, an attempt to measure the dispersion of optical rotation in TA crystals using a WS-HAUP equipment (wavelength-scanning high-accuracy universal polarimeter) built in Oxford (Moxon and Renshaw 1990) was unsuccessful. This technique is rather slow (a single scan takes about two days) which causes a problem for TA cuts as their surfaces deteriorate because of humidity. Furthermore, because of the high birefringence of TA crystals, the samples have to be prepared as very thin plates of thickness less than 0.1 mm, thus increasing the deteriorating effect of the surfaces. The result is that with the WS-HAUP the results tend to be conflicting and variable.

0953-8984/97/4910829+14$19.50

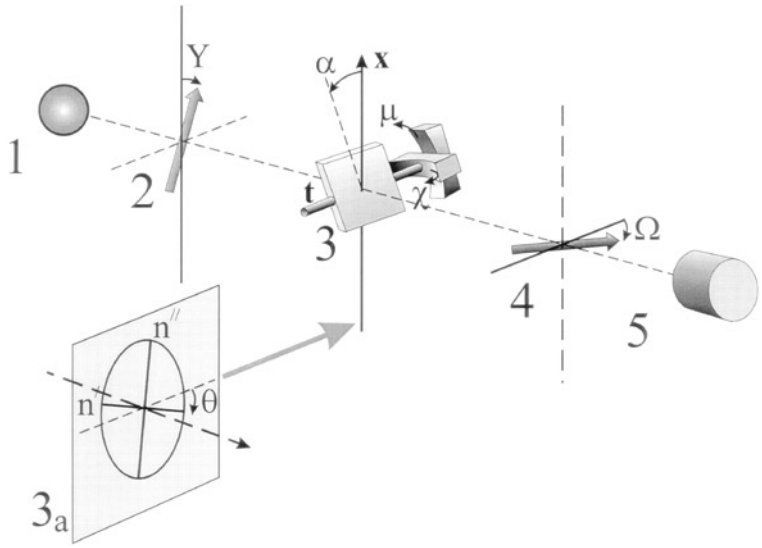

Figure 1. The set-up of the tilter-system. (1) Laser diode, (2) polarizer, (3) tilt axis, (3a) shape of the optical-indicatrix section, (4) analyser system: quarter-wave plate, Pockels modulator ($NH_4H_2PO_4$ single crystal cut on (001) with transparent electrodes) analyser, (5) detector.

Recently, the 'tilter' method was developed (Kaminsky and Glazer 1996). This is also based on the HAUP technique, but here a plane-parallel cut sample plate is tilted about an axis perpendicular to the incident light wave. Furthermore, a fixed wavelength is used. The new system allows the use of a laser and fast light-intensity measurements, whilst the retardation is changed by the tilting. In this way the time for a complete scan can be reduced, typically to 5 min.

Early results obtained with the tilting system have already been published (Kaminsky and Glazer 1997, Kaminsky 1996). Meanwhile, an algorithm has been developed which allows us to derive simultaneously both rotatory power and optical indicatrix orientation from the experimental data by Fourier analysis. In this paper, details of the tilter method, as they apply to low symmetry and high birefringence crystals like TA, and the new algorithm are discussed, and the results of measurements of TA crystals are given.

2. The tilter method

A schematic diagram of the tilting apparatus is shown in figure 1. Although most of the details of the method have been described earlier (Kobayashi and Uesu 1983, Kaminsky 1994, Kaminsky and Glazer 1996) it is worth discussing here the equations underlying the tilter method and their application to TA crystals.

In the tilting system the intensity I_0 of the incident linear-polarized light is approximately related, according to equation (1), to the intensity I resulting from light interaction with the following sequence: polarizer (at angle $Y + 90^\circ$), sample (with angle of extinction θ), and analyser (at angle Ω). The angles are measured with respect to the tilt axis, which is perpendicular to the wavevector.

$$\frac{I}{I_0} \approx (\varphi + \Omega)^2 + (\varepsilon + \varepsilon_A)^2 \tag{1}$$

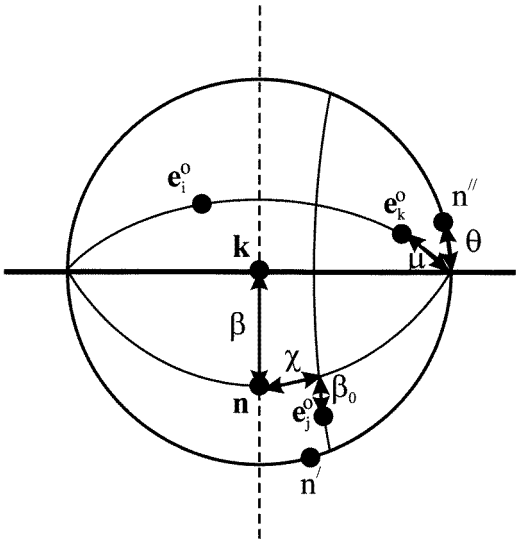

Figure 2. Stereographic projection showing the orientation of the indicatrix with respect to the wavevector $\boldsymbol{k}$ and the tilt axis (bold line). $\boldsymbol{n}$ is the plate-normal vector, $\boldsymbol{e}_i^\circ, \boldsymbol{e}_j^\circ, \boldsymbol{e}_k^\circ$ denote the principal axes of the indicatrix, β is the tilt angle, n' and n'' are vibration modes of the incident wave ($\Delta n = n'' - n'$), θ is the extinction angle and β_0, μ and χ define the orientation of the indicatrix with respect to the wavevector and tilt axis.

where

$$\varphi \approx \varphi_0 \frac{\sin\delta}{\delta} + Y\cos\delta + 2\theta\sin^2\frac{\delta}{2} + \varepsilon_P \sin\delta$$

$$\varepsilon \approx \frac{2\varphi_0}{\delta}\sin^2\frac{\delta}{2} + (Y-\theta)\sin\delta - \varepsilon_P\cos\delta.$$

In equation (1) φ is the azimuthal angle of rotation with respect to the initial light polarization, ε is the ellipticity of the sample, optical rotation $\varphi_0 = L$ (plate thickness) multiplied by ρ (rotatory power), ε_A and ε_P are the parasitic ellipticity of the analyser and polarizer, respectively, and $\delta = 2\pi L\Delta n/\lambda$ is the retardation. Equation (1) is derived on the assumption that all angular quantities, with the exception of φ_0, are small.

Depending on the values of the diagonalized polarization tensor $\{a_{ij}\}$, defined from the Maxwell relation $\varepsilon_0 E_i = a_{ij} D_j$, the extinction direction of a cross section perpendicular to the wavevector $\boldsymbol{k}$ is inclined to the analyser (at $\Omega = 0$) by the angle θ, defined according to equation (2) (Kaminsky 1994):

$$\tan 2\theta = 2\frac{(a_{kk} - a_{jj})\chi\sin\beta + (a_{kk} - a_{ii})\mu\cos\beta}{a_{kk} - a_{jj}\sin^2(\beta - \beta_0) - a_{ii}\cos^2(\beta - \beta_0)} \tag{2}$$

where β and β_0 are the tilt-angle 'inside the sample' ($\sin\beta = \sin\alpha/n_k$, α is the tilt angle of the sample plate) and its offset with respect to the wavevector, respectively; μ and χ angles describe the orientation of the indicatrix with respect to the wavevector and the tilt axis (figure 2).

Equation (1) can be rewritten in the form of a polynomial expression, as shown by Kaminsky and Glazer (1996):

$$\frac{I}{I_0} = a_0 + a_1\Omega + a_2 Y + a_3\Omega Y + \Omega^2 + Y^2 \tag{3}$$

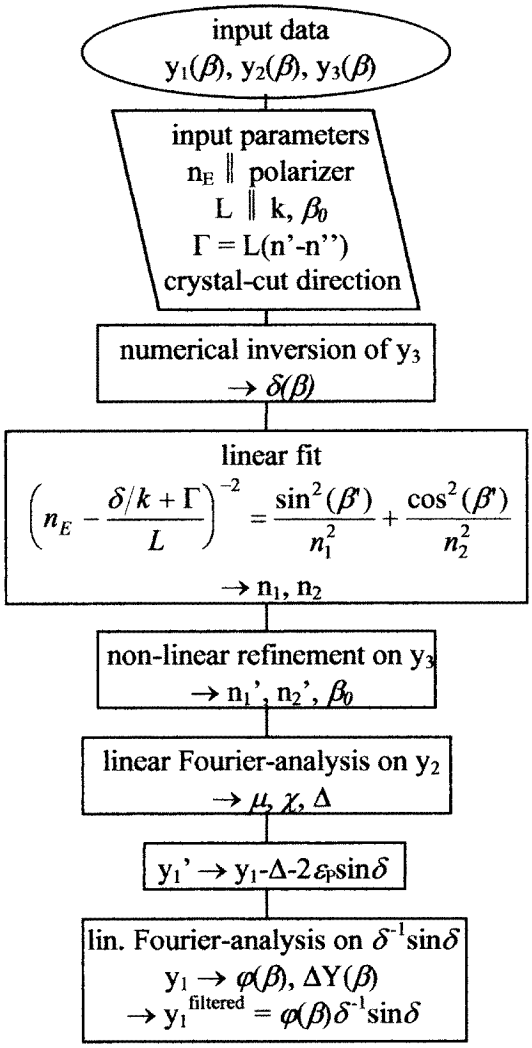

Figure 3. Flow-chart of the data-analysing program. Input data are derived from a fit of the experimental data to the intensity surface, according to equation (3); input parameters: retardation Γ of the crystal cut, orientation of the cut and one refractive index n_E in the direction of the initial polarization; output: refined principal refractive indices in relation to n_E, indicatrix orientation (β_0, χ, μ), the rotatory power along the plate normal $\boldsymbol{n}$, rotatory power perpendicular to $\boldsymbol{n}$ and the tilt axis, and the ellipticity $y_1^{\text{filtered}} = \varphi_0(\beta)\delta^{-1}(\beta)\sin\delta(\beta)$.

where

$$a_1 = 2\left(\frac{\varphi_0}{\delta} + \varepsilon_P\right)\sin\delta + 2\theta(1-\cos\delta)$$
$$a_2 = 2\left(\frac{\varphi_0}{\delta} + \varepsilon_A\right)\sin\delta - 2\theta(1-\cos\delta)$$
$$a_3 = 2\cos\delta$$

and φ_0, θ and δ are all functions of β.

In the tilting method the resulting intensity I is measured for successive β angles as a function of Y and Ω, and then equation (3), which defines a surface in three-dimensional space (I, Y and Ω), is fitted to the experimental points (typically for each tilt angle β about one hundred experimental points are collected within the ranges $-0.7^\circ < Y < 0.7^\circ$ and $-0.7^\circ < \Omega < 0.7^\circ$).

It is useful to define functions $y_1(\beta)$, $y_2(\beta)$ and $y_3(\beta)$ in such a way that $y_1(\beta)$ consists of the gyration-related signal generated from $a_1(\beta) + a_2(\beta)$, i.e. it contains $(\varphi(\beta)\delta^{-1} +$

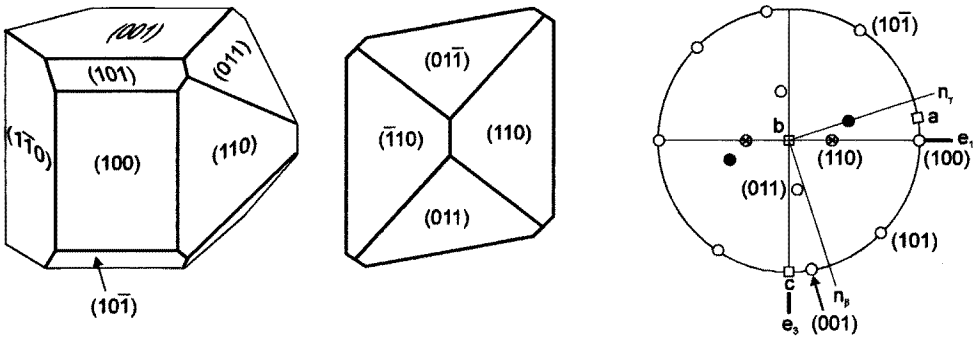

(*a*) (*b*) (*c*)

Figure 4. The habit of a $(2R, 3R)$-TA crystal (*a*) clinographic projection, (*b*) projection along two-fold axis; (*c*) stereographic projection. e_i denotes the physical reference system, n_γ is the acute bisectrix, [010] is parallel to the obtuse bisectrix (n_α), polarizations of the refractive indices n_α, n_β and n_γ are along the principal axes of indicatrix $e_1^\circ, e_2^\circ, e_3^\circ$. Miller indices for the crystal faces are given in brackets. The optic axes are marked by ●.

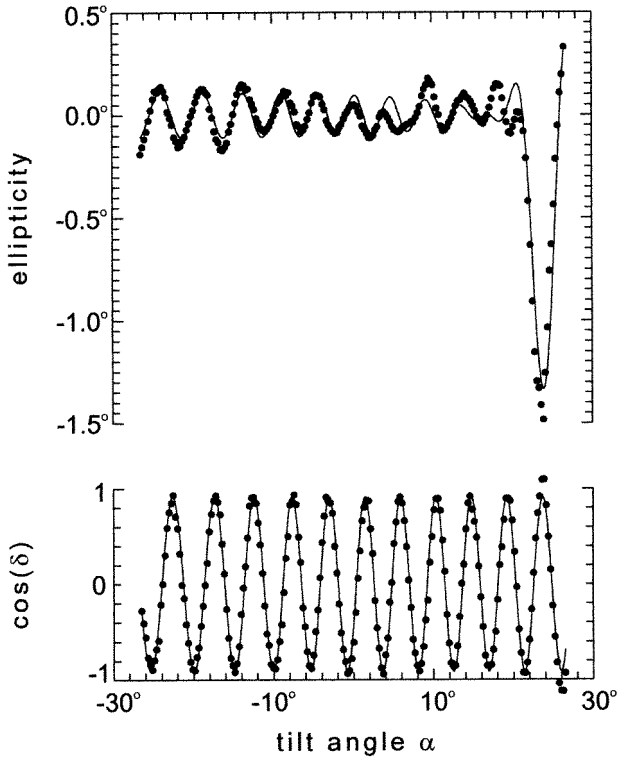

Figure 5. Tilt scan and fit of the ellipticity $\varphi_0(\beta)\sin[\delta(\beta)]/\delta(\beta)$ and $\cos[\delta(\beta)]$, where $\sin\beta = \sin\alpha/n_k$, for sample plate cut almost perpendicular to one of the optic axes (plate 4). Sample thickness = 0.130(5) mm. The wavevector was tilted about e_2°, which is parallel to the polarization of n_β. The optical rotation changes sign for a tilt angle of about 17°, for which the wavevector is 3° inclined towards the optic axis. The continuous lines were calculated according to equations (3).

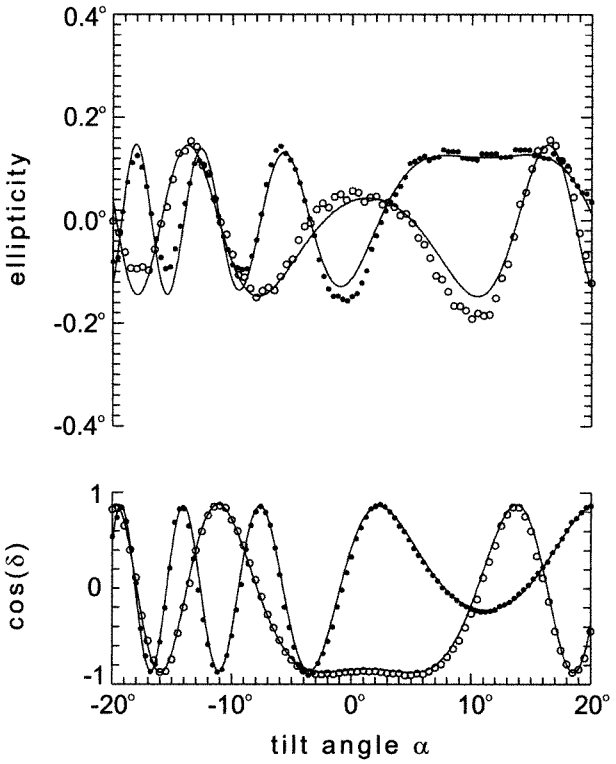

Figure 6. Tilt scan and fit of the ellipticity and $\cos[\delta(\beta)]$ for the cut perpendicular to $\boldsymbol{e}_1^\circ$ (along the polarization of n_α), i.e. for plate 1. Sample thickness = 0.250(5) mm. Experimental results for wavevector tilted towards n_β are marked by ○and for wavevector tilted towards n_γ by ●. Full curves are calculated.

$2\varepsilon_P + \Delta)\sin\delta$. $y_2(\beta)$ is related to $a_1(\beta) - a_2(\beta)$ and depends on $\theta(\beta)[1 - \cos\delta(\beta) + \Delta]$, whereas $y_3(\beta)$ follows the $\cos\delta(\beta)$ distribution. Δ contains the difference between ε_A and ε_P as well as other parasitic ellipticities caused by the reflection and depolarization of the sample. Figure 3 shows schematically a typical analysis of the functions $y_1(\beta)$, $y_2(\beta)$ and $y_3(\beta)$ using as input parameters: retardation of the crystal cut $\Gamma = L(n' - n'')$, where L is the thickness of the sample in the direction of the wavevector $\boldsymbol{k}$ and $(n' - n'')$ represents the double refraction of the section being measured; and orientation of the cut and one refractive index n_E in the direction of the initial polarization. In the first step the numerical inversion of $y_3(\beta)$ into $\delta(\beta)$ is carried out according to the procedure described in the appendix. Assuming that the indicatrix is roughly oriented with one principal direction parallel to the initial polarization, the principal refractive indices n_1 and n_2 in relation to n_E are calculated by a linear fitting procedure, where $\beta' = (\beta - \beta_0)$ and β_0 is not constrained. A further nonlinear refinement of n_1, n_2, and β_0 is carried out using the experimental $y_3(\beta)$. Subsequent analysis of the function $y_2(\beta)$ is able to determine the orientation of the indicatrix and parasitic effects which are related to the adjustment of the analyser and depolarizing effects of the crystal. Finally, the analysis of $y_1(\beta)$ allows us to eliminate the polarizer ellipticity ε_P and sum of the parasitic effects (Δ and ΔY, which is an error caused mainly by the offset in Y of the polarizer). The output of the program contains the refined principal refractive indices in relation to n_E, indicatrix orientation (β_0, χ, μ) rotatory

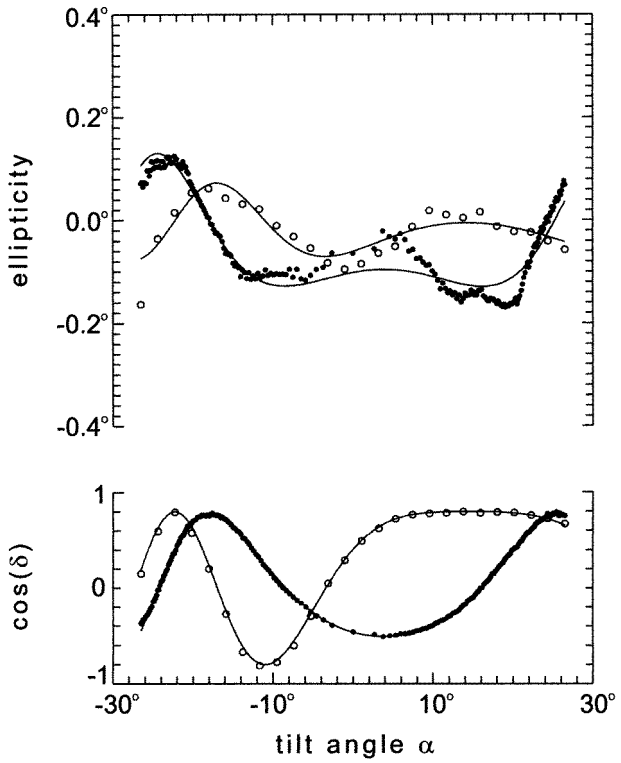

Figure 7. Tilt scan and fit of the ellipticity and $\cos[\delta(\beta)]$ for the cut perpendicular to $\boldsymbol{e}_2^\circ$ (along the polarization of n_β), i.e. for plate 2. Sample thickness = 0.290(5) mm. Experimental results for wavevector tilted towards n_γ are marked by ○and for wavevector tilted towards n_α by ●. Full curves are calculated.

power along the plate normal $\boldsymbol{n}$, rotatory power perpendicular to $\boldsymbol{n}$ and the tilt axis, and the ellipticity $y_1^{\text{filtered}} = \varphi_0(\beta)\delta^{-1}(\beta)\sin\delta(\beta)$.

It is interesting to note that this method is independent of the parasitic ellipticity of the analyser system as well as of the parasitic ellipticity of the sample, whatever its origin.

3. Experimental results

3.1. Optical measurements

Figure 4 shows the habit of the TA crystal used in our experiment and its stereographic projection. The directions of the main refractive indices n_β and n_γ, are marked against the orientation of the Cartesian ($\boldsymbol{e}_1$ and $\boldsymbol{e}_3$) and monoclinic ($\boldsymbol{a}$ and $\boldsymbol{c}$) systems. The orientation of the physical reference system is defined by the following convention: $\boldsymbol{e}_2 \parallel \boldsymbol{b}^*$ (in TA $\boldsymbol{b}^* \parallel \boldsymbol{b}$), $\boldsymbol{e}_3 \parallel \boldsymbol{c}$ and $\boldsymbol{e}_1 = \boldsymbol{e}_2 \times \boldsymbol{e}_3$ ($\boldsymbol{e}_1 \parallel \boldsymbol{a}^*$ in TA), where $\boldsymbol{a}$, $\boldsymbol{b}$, $\boldsymbol{c}$ are crystallographic basis vectors of the direct lattice and $\boldsymbol{a}^*$, $\boldsymbol{b}^*$, $\boldsymbol{c}^*$ are those of the reciprocal lattice. $\boldsymbol{e}_1$ is inclined about 18° clockwise to the polarization of n_γ according to Des Cloizeaux (Groth 1910). X-ray precession photographs confirmed this angle.

All samples of TA were cut from one single crystal (grown from aqueous solution) using a wet wire saw and then prepolished with 5 μm-Al_2O_3 powder. Finally, the plate faces were polished on pitch with Cr_2O_3 (polish-green) while moisture introduced by breathing

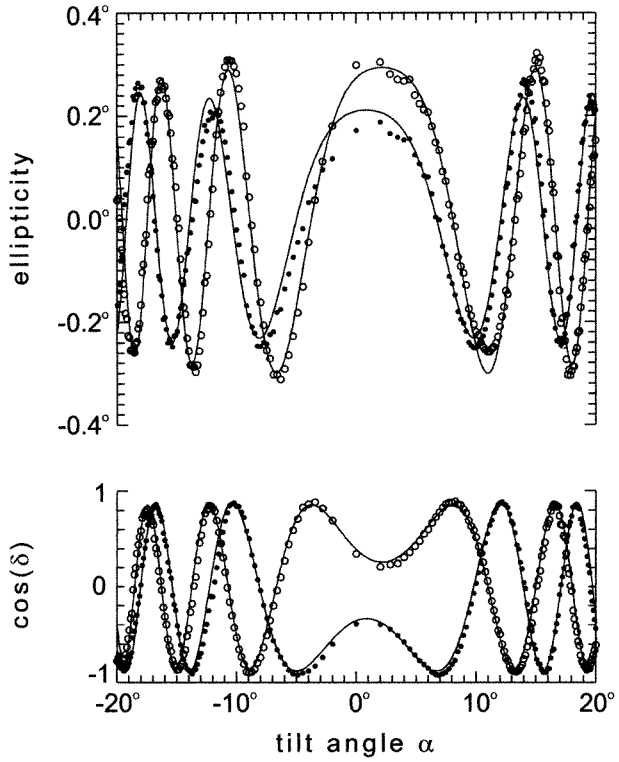

Figure 8. Tilt scan and fit of the ellipticity and $\cos[\delta(\beta)]$ for the cut perpendicular to $\boldsymbol{e}_3^\circ$ (along the polarization of n_γ), i.e. for plate 3. Sample thickness = 0.360(5) mm. Experimental results for wavevector tilted towards n_β are marked by ○and for wavevector tilted towards n_α by ●. Full curves are calculated.

on the pitch-lap helped to establish clear surfaces of optical quality with an inclination less than 2 μm cm^{-1} to each other. The crystal plates prepared in this way had a cross section of about 4×4 mm^2 and thickness between 0.1 and 0.3 mm.

At the beginning of each measurement with the tilter system, the χ and μ angles (see equation (2) and figure 2) were minimized manually by making a test scan. The final scans were performed for six plates of different orientations and the results are shown in figures 5–9. They allowed us to build up an over-determined system of equations. The plates 1, 2 and 3 were cut perpendicular to the vibration of n_α (obtuse bisectrix), n_β (optic-axis normal) and n_γ (acute bisectrix), respectively. Plate number 4 was cut approximately perpendicular to one of the optic axes. Plates 5 and 6 were cut perpendicular to a direction inclined 45° anticlockwise and 45° clockwise against the normal n_γ (see figure 4).

After each complete tilt scan the sample was rotated through 90° about the direction of the incident light and the whole measurement procedure was repeated. In order to improve the elimination of parasitic ellipticities of the set-up (Moxon and Renshaw 1990) the average result for both orientations was taken for further calculations†. The results of the subsequent calculations for six plates allowed all gyration tensor components of the TA crystal to be determined, and these are given in table 1. The value of optical rotation

† The tilter algorithm is not able to eliminate the parasitic contributions completely, when the signal is not sufficiently modulated by the tilting procedure.

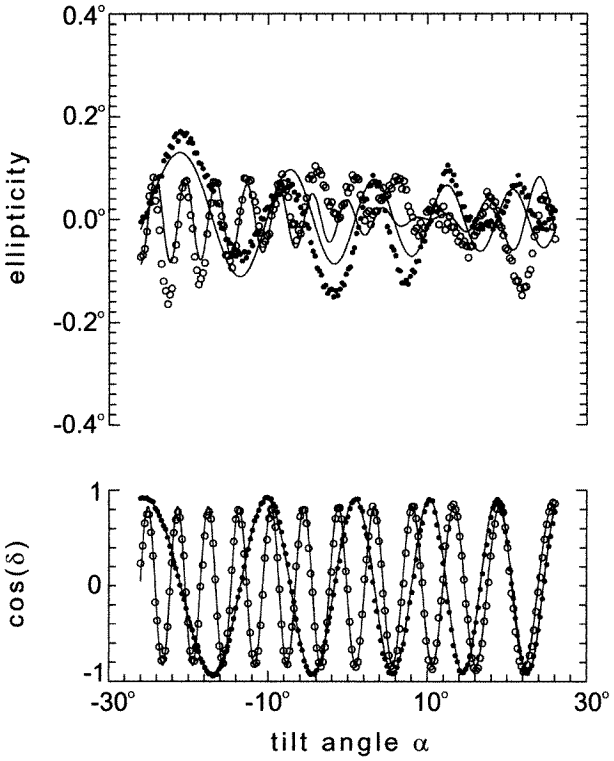

Figure 9. Tilt scan and fit of the ellipticity and $\cos[\delta(\beta)]$ for plate 5 (○, sample thickness = 0.200(5) mm) where optical rotation changes sign, and plate 6 (●, sample thickness = 0.090(5) mm). Full curves are calculated.

along the optic axis itself, found as $-12.3(1.0)^\circ$ mm^{-1} for plate 4, was obtained from the relation: $\rho_{11}^\circ \sin^2\beta' + \rho_{33}^\circ \cos^2\beta'$, where $\beta' = \beta - \beta_0$ and the values of $\rho_{11}^\circ = 65(3)$ and $\rho_{33}^\circ = -62(2)^\circ$ mm^{-1}. These values, although measured with a tilt about a direction close to one of the optic axes, were consistent with those determined independently for plates 1 and 3.

In the calculations the values of retardation for plates 1–6 at a wavelength of 680 nm were obtained using refractive indices which were estimated from the retardations Δ_1 of plate 1 (cut on the acute bisectric) and Δ_2 for one of the 45° cuts (plate 6), both measured directly with an Ehringhaus compensator. The refractive indices were fitted to the tilt-scan data to reproduce the measured birefringence ($n_\gamma - n_\alpha = 0.0932$ and $n_\beta - n_\alpha = 0.0263$)†. The values of refractive indices found in this way are slightly smaller than those expected for a wavelength of 680 nm when compared with the refractive indices measured with the Na D-line (Kohlrausch 1878). The error introduced by this procedure is expected to be smaller than would be found if the Na D-line values or extrapolation values were used instead. The final optical-rotation results are affected by an error of less than 10% which is within the error of the optical-rotation tensor determination.

† In principle, the tilter-method allows us to derive all the principal refractive indices and their polarizations from a single plane-parallel cut sample plate, if its retardation is known.

Table 1. Experimental data for the system of equations describing optical rotation in TA. $\rho(\boldsymbol{k})$ is the optical rotation in the direction of the wavevector $\boldsymbol{k}$. Directions along the principal axes of the indicatrix are marked by $n_\alpha, n_\beta, n_\gamma$. The errors do not include those of systematic origins (i.e. parasitic artefacts, which are eliminated using pairs of measurements as shown in the table). The tensor components in the physical reference system $\{\boldsymbol{e}_i\}$ are: $\rho_{11} = -65(5)$, $\rho_{22} = 79(7)$, $\rho_{33} = 85(12)$, $\rho_{13} = 32(8)^\circ$ mm^{-1}.

Plate no	Direction of $\boldsymbol{k}$	Tilt towards	$\rho(\boldsymbol{k})$ ($^\circ$ mm^{-1})
1	n_α	n_γ	72(3)
	n_α	n_β	94(4)
2	n_β	n_α	60(3)
	n_β	n_γ	115(9)
3	n_γ	n_α	−58(1)
	n_γ	n_β	−74(1)
4	n_α		65(3)
	n_γ		−62(2)
5	45° anticlockwise against n_γ	n_α	−8(10)
6	45° clockwise against n_γ	n_α	28(10)

3.2. Absolute optical chirality

A piece of the original TA crystal was ground to a sphere of diameter 0.42(2) mm and used for absolute structure determination by x-ray diffraction. Intensity measurements were carried out with a KM4 diffractometer (KUMA Diffraction) using graphite-monochromated CuKα radiation. Crystal data: $2R, 3R$-$C_4H_6O_6$, $M_r = 150.09$, monoclinic space group $P12_11$, $a = 7.7238(8)$, $b = 6.0054(4)$, $c = 6.2095(3)$ Å, $\beta = 100.150(8)$, $V = 283.52$ Å^3, $Z = 2$, $D_x = 1.758$ Mg m^{-3}, $\lambda = 1.541\,84$ Å, $\mu = 1.48$ mm^{-1}, $T = 295$ K, $R = 0.0238$ for all 1239 unique reflections, $wR_2(F^2) = 0.0625$, $S = 1.082$, Flack parameter $= -0.05(0.16)$ (Sheldrick 1993). Fractional atomic coordinates and thermal displacements (table 2) were similar to those obtained by Hope and de la Camp (1972)†.

The structural chirality determination for the crystal of class 2 (category I according to Glazer and Stadnicka 1989), which is made possible through the anomalous dispersion of x-rays by the oxygen atoms in general positions, showed unambiguously the absolute configuration of the molecule: $2R, 3R$ (figure 10) for the chiral carbon atoms C(2) and C(3). However, the absolute structure of the crystal can not be defined unless it is linked to an external chiral or polar physical property (see the discussion of Glazer and Stadnicka 1989). Here, we link the structural chirality to the signs of the gyration tensor components measured for the same crystal, which was used for x-ray experiment, thus defining the

† The coordinates x', y', z' equivalent to those published by Hope and de la Camp (1972) can be obtained by the following tranformation:

$$\begin{pmatrix} x' \\ y' \\ z' \end{pmatrix} = \begin{pmatrix} \bar{1} & 0 & 0 \\ 0 & 1 & 0 \\ 0 & 0 & \bar{1} \end{pmatrix} \begin{pmatrix} x \\ y \\ z \end{pmatrix} + \begin{pmatrix} 1 \\ \Delta - \frac{1}{2} \\ \frac{1}{2} \end{pmatrix}$$

where $\Delta = 0.0796$.

Table 2. Fractional atomic coordinates and equivalent isotropic displacement parameters (Å^2), $U_{\rm eq} = \frac{1}{3}\Sigma_i\Sigma_j U_{ij} a_i^* a_j^* \boldsymbol{a}_i \boldsymbol{a}_j$.

Atom	x	y	z	$U_{\rm eq}$
O(11)	0.3910(1)	0.4128(2)	0.1989(2)	0.030(1)
O(12)	0.5707(1)	0.4530(2)	0.5220(2)	0.032(1)
O(2)	0.6620(1)	0.3863(2)	−0.0107(1)	0.028(1)
O(3)	0.6935(1)	0.0016(1)	0.2660(1)	0.023(1)
O(41)	1.0215(1)	0.0123(2)	0.1501(2)	0.040(1)
O(42)	1.0773(1)	0.3398(2)	0.3197(2)	0.036(1)
C(1)	0.5361(1)	0.4259(2)	0.3091(2)	0.021(1)
C(2)	0.7060(1)	0.4044(2)	0.2176(2)	0.020(1)
C(3)	0.7996(1)	0.1926(2)	0.3191(2)	0.019(1)
C(4)	0.9785(1)	0.1679(2)	0.2502(2)	0.023(1)
H(2C)	0.778(2)	0.532(3)	0.264(2)	0.017(3)
H(2O)	0.754(3)	0.416(4)	−0.061(3)	0.047(5)
H(12)	0.468(3)	0.458(4)	0.578(3)	0.044(5)
H(3C)	0.823(2)	0.209(3)	0.473(2)	0.019(3)
H(3O)	0.660(2)	−0.010(3)	0.126(3)	0.034(4)
H(42)	1.171(3)	0.332(4)	0.270(3)	0.057(6)

so-called *absolute optical chirality*.

Additionally, the $(2R, 3R)$ configuration of the molecules in the original TA crystal was examined by measurement of the specific rotation of an aqueous solution with a concentration of 5.6 g per 100 cm^3 (Polamat-A spectropolarimeter, Carl-Zeiss Jena) at room temperature. In the range between 366 and 578 nm $[\alpha]_\lambda^{21\,^\circ\mathrm{C}} = 100\alpha/\mathrm{lc}$ was found to be positive (+5.2 to +15.7° cm^3 dm^{-1} g^{-1}).

4. Discussion

The gyration tensor components for TA crystals of known absolute structure were successfully measured by the tilting method at room temperature for the wavelength 680 nm. We believe that this is the first complete determination of the gyration tensor in a monoclinic crystal. There was an earlier attempt made by Asahi *et al* (1992) as part of an investigation of the optical properties of $BaMnF_4$ using the HAUP method. The measurements were carried out near the phase transition at 250 K, i.e. from the incommensurate pseudo-monoclinic to the orthorhombic phase, both reported to be optically active. The quoted work presents a discussion of the variation of all gyration-tensor components with temperature in the case of low linear birefringence, unfortunately without the elimination of parasitic effects.

Our determination of the gyration tensor components for TA crystals by the tilter method is in good agreement with earlier determinations (Dufet 1907, Longchambon 1924) for the optic axes directions (i.e. for directions with vanishing linear birefringence). A value for the optical rotation, along an optic axis, of 8(5)° mm^{-1} can be calculated from the determined gyration tensor components, assuming $2V = 77.4^\circ$. However, this calculation involves sums and differences of four tensor components and results in a large error for this value. A more reliable estimate is gained by direct measurement along the optic axis: we obtained for this direction a value of 12(1)° mm^{-1}. Both values are nevertheless equivalent within the limit of error to 7.6° mm^{-1} estimated for 680 nm from Longchambon's data using the Chandrasekhar equation (Chandrasekhar 1961) with $K = 2.998 \times 10^6$ ° mm^{-1} nm^{-2} and

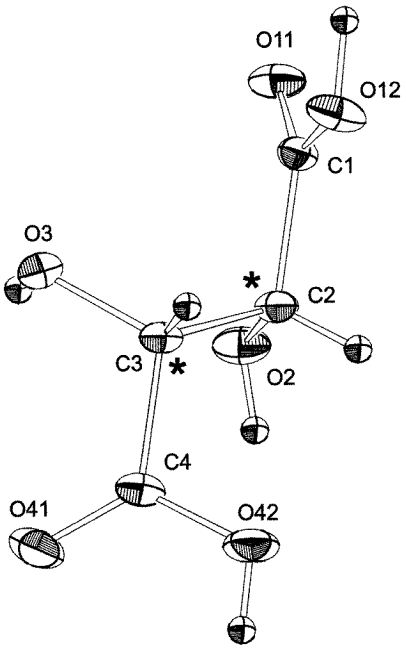

Figure 10. Configuration of the TA molecule (ORTEPII, Johnson 1976). Anisotropic displacement ellipsoids are plotted at the 50% probability level and H atoms are drawn as small circles for clarity.

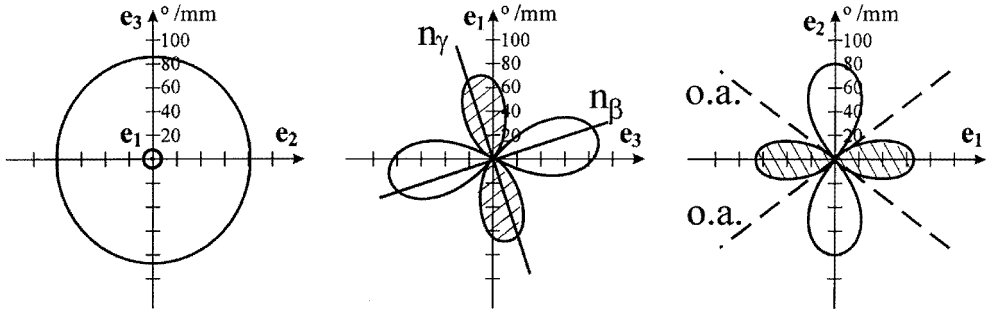

Figure 11. Cross sections of gyration surface in terms of optical rotation for TA crystal at wavelength 680 nm and at room temperature. The shaded area represents the negative optical rotation (right-handed rotation).

$\lambda_0 = 189.7$ nm (λ_0 is in good agreement with the absorption band found by Koralewski and Szafrański (1988) for powdered TA).

The fitting of the principal axes of the gyration tensor components to the experimental data results in the following values: $79(7)^\circ$ mm^{-1} in the direction fixed by the monoclinic two-fold axis, i.e. parallel to the n_α polarization, 92(13) and $-72(4)^\circ$ mm^{-1} in the directions rotated by about 6.5° clockwise with respect to the remaining principal axes of the indicatrix n_β and n_γ, respectively. The rotation angle is rather small, so it is difficult to tell within the limits of error whether the principal directions of the gyration tensor and indicatrix axes $n_\alpha, n_\beta, n_\gamma$ are rotated against each other.

The absolute values of the principal components are an order of magnitude higher than those found for the salts of the tartaric acid, such as uniaxial $Rb_2[(2R, 3R)\text{-}C_4H_4O_6]$ and $Cs_2[(2R, 3R)\text{-}C_4H_4O_6]$ (Stadnicka and Brożek 1991), biaxial Rochelle salt $KNH_4[(2R, 3R)\text{-}C_4H_4O_6] \cdot 4H_2O$ (Kobayashi *et al* 1991) and ammonium Rochelle salt $NaNH_4[(2R, 3R)\text{-}$

$C_4H_4O_6] \cdot 4H_2O$ (Brożek *et al* 1995). The high optical rotation of single-crystal TA is probably due to the three-dimensional network of very strong hydrogen bonds in the crystal structure. We tried to calculate the optical rotation with the program NOPT (Mucha *et al* 1996), which assumes dipole–dipole interactions only, but this was unsuccessful, principally because this computation does not lend itself easily to incorporation of polarizability from hydrogen bonds, nor from intramolecular bonding. In such a case, it is also difficult to adopt a molecular polarizability approach (Munn 1994, Michl and Thulstrup 1986) since the contribution of the molecule itself is relatively small and the hydrogen bonding network closely connects the molecules leading to predominating intermolecular contributions.

Appendix. Numerical inversion of the function $A(\beta)\cos\delta(\beta)$

Consider experimental data $y_3(\beta)$ which represent a function of the type $A(\beta)\cos\delta(\beta)$, where the amplitude $A(\beta)$ is assumed to have negligible variation in comparison with $\cos\delta(\beta)$. A first approximation of the argument $\delta(\beta)$ results from:

$$\delta(r_i < \beta < r_{i+1}) \approx \left(\mathrm{i} + \frac{1}{2}\right)\pi + \arctan\left\{\frac{(r_i - r_{i+1})}{\pi\, y_3(\beta)}\frac{\mathrm{d}y_3(\beta)}{\mathrm{d}\beta}\right\}, \cos(\delta(r_i)) = 0$$

where r_i and $\mathrm{d}y_3(\beta)/\mathrm{d}\beta$ are calculated numerically. The resulting quantities $\delta(\beta)$ are represented by a polynomial expression:

$$\delta'(\beta) = b'_0 + b'_1\beta + b'_2\beta^2 + b'_3\beta^3$$

which is recursively used to obtain

$$\delta'^{+1}(r_j < \beta < r_{j+1}) \approx \left(\mathrm{i} + \frac{1}{2}\right)\pi + \arctan\left\{[(b'_1 + 2b'_2\beta + 3b'_3\beta^2)y_3(\beta)]^{-1}\left(-\frac{\mathrm{d}y_3(\beta)}{\mathrm{d}\beta}\right)\right\} \equiv b'^{+1}_j\beta'_j.$$

The inversion of $A(\beta)\cos\delta(\beta)$ into $\delta(\beta)$ can easily be performed within less than 10 iterations.

Acknowledgments

We thank Dr Marceli Koralewski from UAM Poznań for providing us with a suitable single crystal of TA. DM is grateful to the Faculty of Chemistry, Jagiellonian University, Cracow, and to Jesus College, Oxford, for financial support. WK is grateful to the Deutsche Forschungsgemeinschaft.

References

Asahi T, Tomizawa M, Kobayashi J and Kleemann W 1992 *Phys. Rev.* B **45** 1971
Brożek Z, Stadnicka K, Lingard R J and Glazer A M 1995 *J. Appl. Cryst.* **28** 78
Chandrasekhar S 1961 *Proc. R. Soc.* A **105** 531
Curie J and Curie P 1882 *Z. Krist.* **6** 291
De la Provostaye H 1841 *Ann. Chim. Phys.* **3** 129
Dufet H 1907 *Z. Krist.* **42** 193
Glazer A M and Stadnicka K 1989 *Acta Cryst.* A **45** 234
Groth P 1910 *Chem. Krystallographie* **III** 303
Hope H and de la Camp U 1972 *Acta Cryst.* A **28** 201
Johnson C K 1976 *Report* ORNL-5138, Oak Ridge National Laboratory, TN, USA

Kaminsky W 1994 *Phase Trans.* **52** 235
——1996 *Phase Trans.* **59** 121
Kaminsky W and Glazer A M 1996 *Ferroelectrics* **183** 133
——1997 *Z. Krist.* **212** 283
Kobayashi J, Uchino K and Asahi T 1991 *Phys. Rev.* B **43** 5706
Kobayashi J and Uesu Y 1983 *J. Appl. Cryst.* **16** 204
Kohlrausch S F 1878 *Z. Krist.* **2** 100
Koralewski M and Szafrański M 1988 *J. Mol. Struct.* **174** 411
Longchambon M L 1924 *Séance du Acad. Sci. Paris* **178** 951
Michl J and Thulstrup EW 1986 *Spectroscopy with Polarized Light* (New York: VCH)
Moxon J R L and Renshaw A R 1990 *J. Phys.: Condens. Matter* **2** 6807
Mucha D, Stadnicka K, Glazer A M and Devarajan V 1996 *J. Appl. Cryst.* **29** 304
Munn R W 1994 *J. Chem. Phys.* **100** 6203
Pasteur M L 1849 *Compt. Rend.* **29** 297
Sheldrick G M 1993 *SHELXL93 Program for the Refinement of Crystal Structures* University of Göttingen, Germany
Stadnicka K and Brożek Z 1991 *Acta Cryst.* B **47** 484